according to the Association for Research in Vision and Ophthalmology Statement for the Use of Animals in Ophthalmic and Vision Research and the National Institutes of Health policies on the Care and Use of Laboratory Animals.

The rabbits were anesthetized with an intramuscular injection of ketamine hydrochloride (32 mg/kg body weight) and xylazine hydrochloride (4 mg/kg body weight). Two scleral incisions were made in the inferotemporal quadrant and superonasal quadrant 1.5 mm from the limbus in the left eye. A 20-gauge infusion cannula was sutured at the incision in the inferotemporal quadrant, and a lensectomy was performed with a cutter through the scleral incision in the superonasal quadrant. Using a contact lens, a two-port vitrectomy was performed and perfluorocarbon liquid was injected to fill the vitreous cavity. Another 7 mm scleral incision was made 1.5 mm posterior to the limbus, and the Teflon trocar was inserted and positioned in the incision. The electrode device was inserted into the vitreous cavity through the trocar. Only the trocar was removed from the incision, which then was sutured with 8-0 Vicryl. The perfluorocarbon liquid then was aspirated. The rod for manipulation and fixation was grasped with a vitreoretinal forceps, and the electrode tips were inserted while the rod was manipulated.

Electrically evoked potential at the visual cortex with electrical stimulation

We determined if the electrically evoked potentials (EEPs) induced by electrical stimulation through the electrodes in the device could be recognized in a rabbit as previously described [19]. The induced EEPs were recorded after implantation of the electrode device to examine activation of the device. Following anesthesia, an incision was made in the top of the scalp, the surface membrane of the skull was removed, and the skull was exposed. The forehead above the visual cortex was drilled in two places 8 mm from the sutura lambdoidea, 7 mm to the right and left of the meridian. Screw-type silver-coated stainless electrodes were screwed into the skull to attach to the dura mater. The reference electrode was placed on the midline 15–20 mm anterior to the lambdoid suture. The extraocular ends of each of the six stimulating electrodes and one reference electrode were connected to the stimulus isolation unit (SIU-A365, World Precision Instruments, Sarasota, FL, USA) of a stimulator (SEN-7203, Nihon Kohden, Tokyo, Japan), allowing electrical pulses to be delivered to six different pairs of electrodes. Biphasic, current-balanced rectangular pulses with an initial cathodic pulse were used. The pulse duration was 0.25 ms, the current 500 μA, and 50 cortical responses were averaged and displayed on a digital storage oscilloscope (Neuropack 2, MEB-7202, Nihon Kohden).

Results

Surgical procedures to implant the electrode device

In the porcine study, during insertion of the electrode device into the vitreous cavity through a 5 mm scleral incision, the electrode tips bent and the device could not be inserted smoothly. We then used a trocar to allow the device to insert into the vitreous cavity in subsequent eyes. After a 7 mm scleral incision had been made, the trocar was positioned at the scleral incision and the device could be inserted smoothly into the vitreous cavity through the trocar without bending the electrode tips.

In the rabbit eyes, hemorrhaging from the incision occurred when the 7 mm scleral incision was made, and was stopped by diathermy. Some hemorrhaging was seen in the subretinal space of each rabbit. Perfluorocarbon liquid was injected to fill the vitreous cavity after the vitrectomy, and the device was inserted into the vitreous cavity using the trocar with the 7 mm scleral incision. The electrode device was implanted into the optic nerve using vitreoretinal forceps (Fig. 2) (Synergetics, Inc., St. Charles, MO, USA) during a single insertion. The positioning of the electrode device into the optic disc was performed smoothly within 10 min. No complications developed during implantation of the device.

Electrically evoked potential at the visual cortex with electrical stimulation

When electrical stimulation was applied between the reference electrode and each of the six stimulating electrodes, the EEPs were recorded from all electrode pairs with an epidural electrode (Fig. 3). The ranges for the implicit time of the first positive peak of the EEP when the stimulation range was 500 μA were similar among the electrode pairs (mean 14.3 ± 0.5 ms). The peak-to-peak amplitudes of the EEPs were 335.1–948.5 μV (mean 782.6 ± 233.7).

Discussion

In the current study, when the trocar was used, the electrode tips were undamaged during insertion into the vitreous cavity. We easily manipulated the electrode device and smoothly and steadily inserted the electrode tips into the optic nerve disc. The electrode device was set into the optic disc in one step within 10 min. This device minimized damage to the optic disc without repeated insertion of the

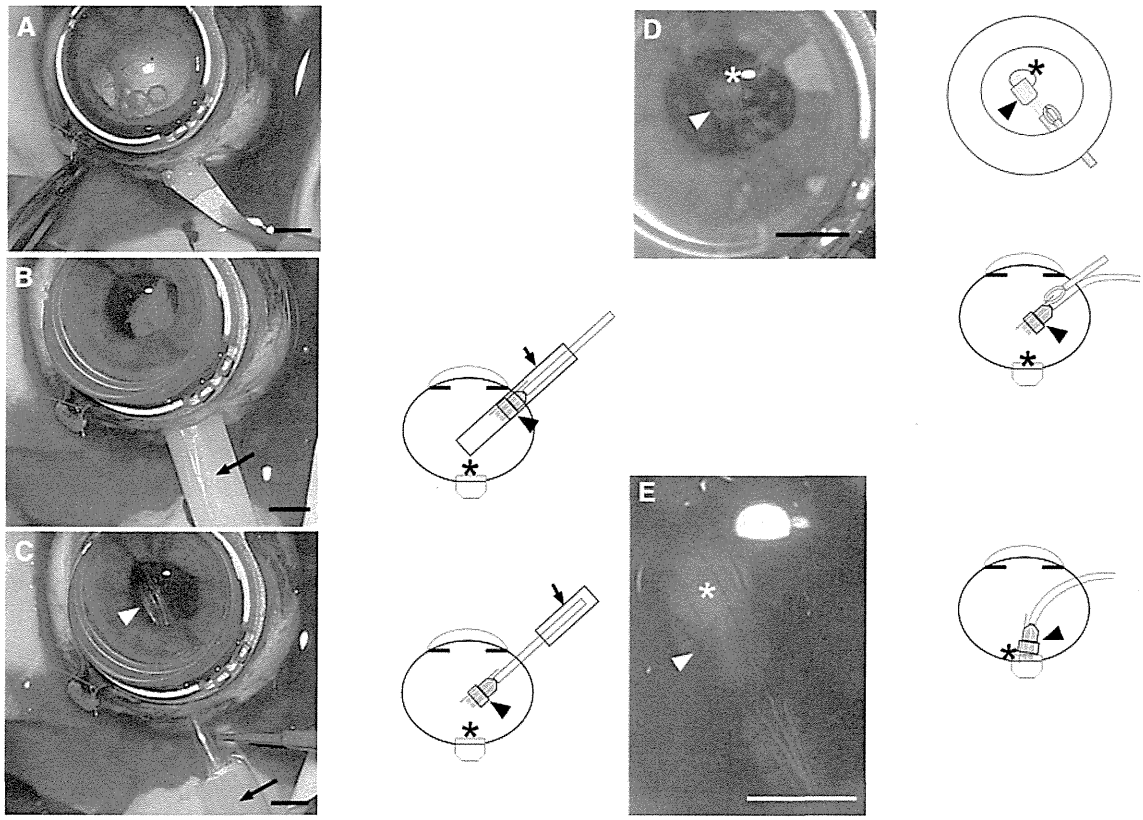

Fig. 2 Electrode implantation. The drawings to the *right* of the surgical view indicate the maneuvers in each step of the procedure. The *arrow*, the *arrowhead*, and the *asterisk* indicate the trocar, the electrode device, and the optic disc, respectively. **a** After a lensectomy and a two-port vitrectomy has been performed and perfluorocarbon liquid has been injected to fill the vitreous cavity, a 7 mm scleral incision is made 1.5 mm posterior to the limbus using an ophthalmic surgical knife. **b** A Teflon trocar is inserted and positioned in the scleral incision. **c** The electrode device is inserted into the vitreous cavity through the trocar. Only the trocar is removed from the incision. **d** The manipulation rod is grasped easily with standard 20-gauge asymmetric vitreoretinal forceps in the vitreous cavity. The drawings show schematic and cross-section views, respectively. **e** The tips of the electrodes and the rod are inserted into the optic nerve disc. *Scale bar* 2 mm

electrodes, allowed the fixation of more electrodes, and shortened the surgical time. Perfluorocarbon liquid in the vitreous cavity prevented ocular collapse during the surgical procedures, even though the incision was 7 mm wide. Thus, the surgical procedures performed using the direct optic nerve electrode device, the trocar, and perfluorocarbon liquid were useful for inducing the artificial vision system into the eyes.

No severe complications developed during any surgical procedures in this animal study. However, hemorrhaging from the incision occurred when the 7 mm scleral incision was made. Although the bleeding was stopped by diathermy, some hemorrhaging was seen in the subretinal space of each rabbit. In our previous clinical study of direct optic nerve electrode implantation in a blind patient with RP [22], when a scleral incision of about 6 mm was made to insert the electrode wire bundle, hemorrhaging was minimal from the sclera and uvea. The hemorrhage was much less than in rabbit eyes and was easily stopped with diathermy.

Based on the results reported by Belgian researchers, four electrodes seemed sufficient to induce artificial vision that targeted electrical stimulation of the optic nerve fibers [11, 12]. The group, which implanted a spiral-cuff electrode comprising four electrodes around the optic nerve behind the eyeball of a blind patient, reported that the phosphene positions changed with electrical stimulation through the same electrode when the stimulation parameters (pulse width, current intensity, number, and frequency) were changed. However, an increased number of electrodes might be advantageous for inducing increased resolution power. With an animal study, it is impossible to examine the resolving power and the width of the visual field, which was the limitation of our current study.

We tested the electrical stimulation of the optic nerve with wire-type electrodes inserted transvitreously as an alternative to conventional visual prostheses. The efficacy and safety of this system have been reported in acute and long-term animal studies [19–21]. We also evaluated the usefulness and safety of our system during a preliminary

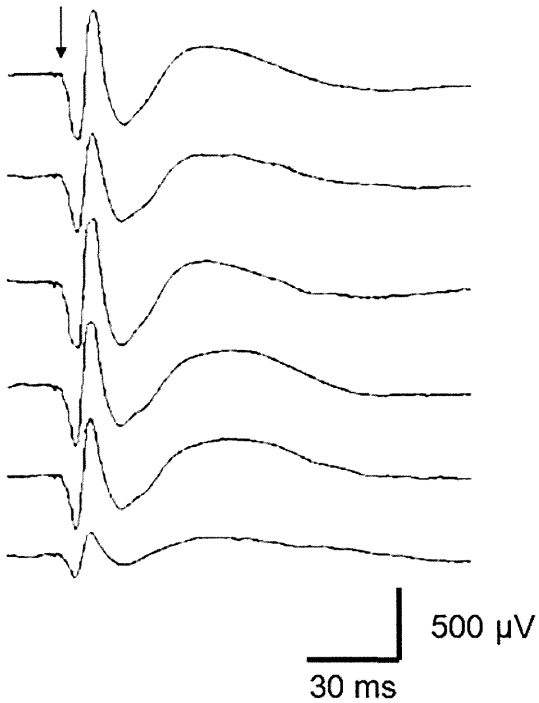

Fig. 3 The EEPs elicited from the six pairs of electrodes are obtained with electrical stimulation through each of six stimulation electrodes and one reference electrode. The *arrow* indicates the time point of electrical stimulation

clinical trial in a blind patient with RP with a long follow-up period of 9 months. In the current study, we demonstrated the surgical procedures needed to implant a newly developed direct optic nerve electrode device into the optic disc. To use this device in blind individuals, safety precautions are needed for long-term electrode placement in the eyes. Rabbit eyes are relatively small in volume compared to human eyes. Thus, we may need other larger animals, such as dogs [16] or monkeys, for future studies. We believe that this electrode device is an important step toward realizing our goal of providing a prosthesis that will benefit blind patients.

Acknowledgments This study was supported by a Grant-in-Aid for Scientific Research (A) from the Japan Society for the Promotion of Science, Japan, and a Health Sciences Research Grant from the Ministry of Health, Labor and Welfare, Japan. The authors appreciate the leadership of the late Professor Yasuo Tano, chairman of the Department of Ophthalmology, Osaka University Graduate School of Medicine, who planned and guided the Artificial Vision projects.

References

1. Brindley GS, Lewin WS. The sensations produced by electrical stimulation of the visual cortex. J Physiol. 1968;196:479–93.
2. Dobelle WH, Mladejovsky MG, Girvin JP. Artificial vision for the blind: electrical stimulation of visual cortex offers hope for a functional prosthesis. Science. 1974;183:440–4.
3. Humayun MS, de Juan E, Weiland JD Jr, Dagnelie G, Katona S, Greenberg R, Suzuki S. Pattern electrical stimulation of the human retina. Vis Res. 1999;39:2569–76.
4. Humayun MS, Weiland JD, Fujii GY, Greenberg R, Williamson R, Little J, Mech B, Cimmarusti V, Van Boemel G, Dagnelie G, de Juan E. Visual perception in a blind subject with a chronic microelectronic retinal prosthesis. Vis Res. 2003;43:2573–81.
5. Chow AY, Chow VY. Subretinal electrical stimulation of the rabbit retina. Neurosci Lett. 1997;225:13–6.
6. Zrenner E, Miliczek KD, Gabel VP, Graf HG, Guenther E, Haemmerle H, Hoefflinger B, Kohler K, Nisch W, Schubert M, Stett A, Weiss S. The development of subretinal microphotodiodes for replacement of degenerated photoreceptors. Ophthalmic Res. 1997;29:269–80.
7. Zrenner E, Stett A, Weiss S, Aramant RB, Guenther E, Kohler K, Miliczek KD, Seiler MJ, Haemmerle H. Can subretinal microphotodiodes successfully replace degenerated photoreceptors? Vis Res. 1999;39:2555–67.
8. Zrenner E. Will retinal implants restore vision? Science. 2002; 295:1022–5.
9. Rizzo JF III, Wyatt J, Humayun M, de Juan E, Liu W, Chow A, Eckmiller R, Zrenner E, Yagi T, Abrams G. Retinal prosthesis: an encouraging first decade with major challenges ahead. Ophthalmology. 2001;26:13–4.
10. Rizzo JF III, Wyatt J, Loewenstein J, Kelly S, Shire D. Methods and perceptual thresholds for short-term electrical stimulation of human retina with microelectrode arrays. Invest Ophthalmol Vis Sci. 2003;44:5355–61.
11. Veraart C, Raftopoulos C, Mortimer JT, Delbeke J, Pins D, Michaux G, Vanlierde A, Parrini S, Wanet-Defalque MC. Visual sensations produced by optic nerve stimulation using an implanted self-sizing spiral cuff electrode. Brain Res. 1998;813:181–6.
12. Veraart C, Wanet-Defalque MC, Gerard B, Valierde A, Delbeke J. Pattern recognition with the optic nerve visual prosthesis. Artif Organs. 2003;27:996–1004.
13. Sakaguchi H, Fujikado T, Fang X, Kanda H, Osanai M, Nakauchi K, Ikuno Y, Kamei M, Yagi T, Nishimura S, Ohji M, Yagi T, Tano Y. Transretinal electrical stimulation with a suprachoroidal multichannel electrode in rabbit eyes. Jpn J Ophthalmol. 2004;48:256–61.
14. Nakauchi K, Fujikado T, Kanda H, Morimoto T, Choi JS, Ikuno Y, Sakaguchi H, Kamei M, Ohji M, Yagi T, Nishimura S, Sawai H, Fukuda Y, Tano Y. Transretinal electrical stimulation by an intrascleral multichannel electrode array in rabbit eyes. Graefes Arch Clin Exp Ophthalmol. 2005;243:169–74.
15. Fujikado T, Morimoto T, Kanda H, Kusaka S, Nakauchi K, Ozawa M, Matsushita K, Sakaguchi H, Ikuno Y, Kamei M, Tano Y. Evaluation of phosphenes elicited by extraocular stimulation in normals and by suprachoroidal–transretinal stimulation in patients with retinitis pigmentosa. Graefes Arch Clin Exp Ophthalmol. 2007;245:1411–9.
16. Morimoto T, Kamei M, Nishida K, Sakaguchi H, Kanda H, Ikuno Y, Kishima H, Maruo T, Konoma K, Ozawa M, Nishida K, Fujikado T. Chronic implantation of newly developed suprachoroidal–transretinal stimulation prosthesis in dogs. Invest Ophthalmol Vis Sci. 2011;52:6785–92.
17. Fujikado T, Kamei M, Sakaguchi H, Kanda H, Morimoto T, Ikuno Y, Nishida K, Kishima H, Maruo T, Konoma K, Ozawa M, Nishida K. Testing of semichronically implanted retinal prosthesis by suprachoroidal–transretinal stimulation in patients with retinitis pigmentosa. Invest Ophthalmol Vis Sci. 2011;52: 4726–33.
18. Santos A, Humayun MS, de Juan E, RJ Greenburg Jr, Marsh MJ, Klock IB, Milam AH. Preservation of the inner retina in retinitis pigmentosa. A morphometric analysis. Arch Ophthalmol. 1997; 115:511–5.

19. Sakaguchi H, Fujikado T, Kanda H, Osanai M, Fang X, Nakauchi K, Ikuno Y, Kamei M, Ohji M, Yagi T, Tano Y. Electrical stimulation with a needle-type electrode inserted into the optic nerve in rabbit eyes. Jpn J Ophthalmol. 2004;48:552–7.
20. Fang X, Sakaguchi H, Fujikado T, Osanai M, Kanda H, Ikuno Y, Kamei M, Ohji M, Gan D, Choi J, Yagi T, Tano Y. Direct stimulation of optic nerve by electrodes implanted in optic disc of rabbit eyes. Graefes Arch Clin Exp Ophthalmol. 2005;243:49–56.
21. Fang X, Sakaguchi H, Fujikado T, Osanai M, Ikuno Y, Kamei M, Ohji M, Yagi T, Tano Y. Electrophysiological and histological studies of chronically implanted intrapapillary microelectrodes in rabbit eyes. Graefes Arch Clin Exp Ophthalmol. 2006;244: 364–75.
22. Sakaguchi H, Kamei M, Fujikado T, Yonezawa E, Ozawa M, Cecilia-Gonzalez C, Ustariz-Gonzalez O, Quiroz-Mercado H, Tano Y. Artificial vision by direct optic nerve electrode (AV-DONE) implantation in a blind patient with retinitis pigmentosa. J Artif Organs. 2009;12:206–9.
23. Nishida K, Sakaguchi H, Xie P, Terasawa Y, Ozawa M, Kamei M, Nishida K. Biocompatibility and durability of Teflon-coated platinum–iridium wires implanted in the vitreous cavity. J Artif Organs. 2011;14:357–63.

Vitrectomy without Laser Treatment or Gas Tamponade for Macular Detachment Associated with an Optic Disc Pit

Akito Hirakata, MD,[1] Makoto Inoue, MD,[1] Tomoyuki Hiraoka, MD,[1] Brooks W. McCuen II, MD[2]

Purpose: To evaluate the clinical outcomes after vitrectomy, without gas tamponade or laser photocoagulation to the margin of the optic nerve, for the treatment of macular detachment associated with optic disc pits and to characterize retinal manifestations during treatment of optic pit maculopathy using optical coherence tomography (OCT).

Design: Noncomparative, retrospective, interventional case series.

Participants: Eight consecutive patients (8 to 56 years of age) with unilateral macular detachment associated with optic disc pit.

Intervention: Pars plana vitrectomy with induction of a posterior vitreous detachment (PVD) was performed in all eyes. No laser or gas injection was performed in any eye during the original surgery. Patients were followed up for 10 to 46 months (mean, 26 months) after surgery.

Main Outcome Measures: Anatomic outcome as determined by OCT and postoperative visual acuities were the main outcome parameters. Fundus autofluorescence (FAF) images were obtained in 4 eyes to document anatomic changes in the macula.

Results: Although complete retinal reattachment was achieved in 7 of 8 eyes, up to about 1 year was necessary for the retinal detachment to resolve fully. The 1 eye in which macular detachment failed to resolve completely underwent revision of vitrectomy with a gas tamponade and laser photocoagulation in the peripapillary area. In the early postoperative period, despite persistent macular detachment, the visual acuities improved in 7 eyes. These improved acuities corresponded with remodeling of the photoreceptor outer segments on OCT and the appearance of granular hyperfluorescence on FAF imaging.

Conclusions: Vitrectomy with induction of a PVD at the optic disc without gas tamponade or laser photocoagulation seems to be an effective method of managing macular detachment resulting from optic disc pits. The OCT scanning before and after surgery suggests that peripapillary vitreous traction with the passage of fluid into the retina through the pit is the cause of the schisis-like separation seen in optic disc pit maculopathy.

Financial Disclosure(s): The author(s) have no proprietary or commercial interest in any materials discussed in this article. *Ophthalmology 2012;119:810–818 © 2012 by the American Academy of Ophthalmology.*

An optic disc pit is a congenital anomaly of the optic nerve frequently associated with macular detachment.[1–4] Optical coherence tomography (OCT) has confirmed the observation of Lincoff et al[5] that there was frequently a retinoschisis-like separation of the retina present during the development of serous macular detachment.[6–8] However, the pathogenesis of optic disc pit maculopathy remains unclear.

The treatment of optic disc pit maculopathy remains controversial. The use of peripapillary laser therapy to produce a barrier of chorioretinal adhesions at the optic disc border with or without intravitreous gas injection often is unsuccessful, and repeated treatments are needed.[9–13] Although Theodossiadis[14] reported that macular scleral buckling can yield favorable anatomic and functional results, this techniques has not been adopted widely. Lincoff et al[15] reported that intravitreal gas injection alone can induce pneumatic displacement of the outer layer detachment and can improve central vision. However, this beneficial effect may be only temporary, because recurrence of macular involvement caused by fluid movement into the subretinal space from persistent inner layer separation has been shown by OCT.[8]

The authors previously reported that the induction of posterior vitreous detachment (PVD) and gas tamponade without laser treatment for optic disc pit maculopathy is effective in reattaching the retina and improving visual acuity.[16] This finding suggested that vitreous traction around the optic disc pit may cause passive fluid migration into the intraretinal space through the pit. Although the ultimate success rate in this series was high, most eyes required almost 1 year to reach complete reattachment after vitrectomy and gas tamponade. Because of the long time necessary for resolution of the subretinal fluid in this series, the authors hypothesized that the gas tamponade may not be necessary for success. Not performing a gas tamponade in these cases allows elimination of the need for prone positioning after surgery, as well as any complications related to fluid–air exchange or gas tamponade. In addition, the early postoperative events are studied better with OCT in the fluid-filled eye compared with the gas-filled eye. The pur-

ISSN 0161-6420/12/$–see front matter
doi:10.1016/j.ophtha.2011.09.026

pose of this study was to evaluate the clinical outcomes in 8 consecutive eyes that underwent vitrectomy with PVD induction without gas tamponade or laser application for the treatment of optic disc pit maculopathy and to characterize the course of retinal reattachment after surgery for optic disc pit maculopathy.

Patients and Methods

Eight eyes of 8 consecutive patients with optic disc pit maculopathy who sought treatment at the Kyorin Eye Center or Duke Eye Center were included in this study. This study had Kyorin University or Duke University Institutional Review Board approval and records were reviewed retrospectively. This clinical study has been registered at the United States National Institutes of Health (www.clinicaltrials.gov) as "Vitrectomy for Optic Disc Pit Maculopathy" with a reference number of NCT01340703. Best-corrected visual acuity (BCVA) was recorded and indirect funduscopy and slit-lamp biomicroscopy using a 90-diopter noncontact lens were performed before and after surgery. The OCT images of the eyes were obtained using Stratus OCT (Carl Zeiss Meditec, Inc., Dublin, CA), OCT 4000 Cirrus (Carl Zeiss Meditec, Inc.), or Spectralis OCT (Heidelberg Engineering, Heidelberg, Germany) to evaluate posterior retinal changes during follow-up. The fundus autofluorescence (FAF) images obtained by confocal scanning laser ophthalmoscopy (cSLO) (Heidelberg Retina Angiograph 2; Heidelberg Engineering) also were evaluated and compared with the ophthalmologic and OCT images beginning in 2009.

Surgery was performed for worsening BCVA or for the development of macular detachment. Surgeries were performed by 3 surgeons (A.H., M.I., or B.W.M.) between 2005 and 2009, and patients were followed up for 10 to 46 months after surgery (mean, 26 months). Vitrectomy was performed with the intention of releasing vitreous traction at the optic disc pit. Twenty-gauge vitrectomy was performed in 3 eyes and 25-gauge vitrectomy was performed in 5 eyes. Posterior vitreous detachment was initiated by suction over the optic disc or near areas of retinoschisis-like separation using the vitreous cutter or microhook. To limit retinal damage secondary to surgical manipulation, special attention was given to separating the posterior hyaloid gently over schisis-like areas. Triamcinolone acetonide was used during surgery to visualize better the posterior cortical vitreous.[17] The internal limiting membrane (ILM) was removed after PVD induction in one patient (patient 8) because the ILM in this patient was separated from the surface of retina before surgery. Neither a gas tamponade nor laser photocoagulation was performed during the primary procedure in any of these cases.

Results

Preoperative Clinical Characteristics

The clinical characteristics of all 8 patients are shown in Table 1, and clinical photographs of representative patients are shown in Figures 1, 2, and 3. Six of the patients were male and 2 were female, with ages ranging from 8 to 56 years (mean, 32.3 years). All patients were of Japanese ethnicity except for patient 3, who was white. All patients reported decreased BCVA, a central scotoma, or metamorphopsia in the affected eye for more than several months. Seven of the affected eyes had no significant refractive error and 1 eye (patient 4) had moderate myopia. The preoperative Snellen BCVA ranged from 20/300 to 20/20 (mean, 20/67). One patient had a chorioretinal coloboma below the optic disc in addition to the optic disc pit (patient 4). No patients had undergone any prior treatment for their optic disc pit maculopathy. The younger two patients (patients 2 and 7) noted their visual disturbance after blunt ocular trauma, when a macular detachment associated with an optic disc pit was diagnosed in the eye. One patient (patient 6) had a medical history of central serous chorioretinopathy treated with laser approximately 20 years previously in the affected eye, but no visible laser scar was apparent. The other 5 patients had no pertinent medical or ocular history.

The presence of a schisis-like separation was confirmed before surgery in 7 of 8 eyes. One patient (patient 3) had macular detachment only. An outer layer schisis-like separation was found in 6 eyes, and multiple shallow inner layer schisis-like separations (edema-like spaces) with or without ILM separation were noted in 5 eyes. Macular retinal detachment (RD) initially was observed in 7 of 8 eyes. This RD did not connect to the optic disc in 5 eyes, but was connected in 2 eyes (patients 3 and 7). Patient 8 had multiple layers of retinal separation, including marked separation of the ILM, but no apparent RD. This patient initially sought treatment with a BCVA of 20/20 and reporting metamorphopsia. One month later, a macular detachment developed with a decrease in the BCVA (Fig 3). The OCT images could not detect any definite communication between the schisis-like separation and vitreous cavity in any of the eyes. Neither PVD nor vitreomacular traction was observed in any of the eyes before surgery by fundus biomicroscopy or OCT scanning.

Anatomic Results

Complete retinal reattachment as determined by OCT images was achieved in 7 of 8 eyes after initial treatment (Figs 1 and 2). No recurrences were observed in these 7 eyes. The other eye (patient 6) showed an initial reduction in the height of the macular detachment with improved BCVA and decreased metamorphopsia over the first few postoperative months, but increased macular elevation developed approximately 10 months after surgery, with the BCVA dropping to 20/200 (Fig 3). An intravitreal gas injection was performed with postoperative prone positioning, but the detachment failed to improve. The patient then underwent revision of vitrectomy with ILM peeling over posterior pole, subretinal fluid drainage, and placement of a gas tamponade. After surgery, submacular fluid with a shallow retinoschisis-like separation recurred. The OCT scans obtained during the recurrence of subretinal fluid showed a relatively high elevation of the retina around a vessel at the margin of the optic disc, leading to application of laser photocoagulation to a small area beside the vessel in the peripapillary region (only 6 laser spots). At 4 months after photocoagulation, the area of RD had shifted superiorly and appeared smaller. The OCT imaging in the peripapillary area revealed a communication between the subretinal fluid and the perivascular area near the optic disc pit (Fig 3). Seven months after photocoagulation, the retinal detachment had resolved, corresponding to an increase in hyperfluorescence on FAF imaging (Fig 3).

Postoperative OCT scanning in the 7 successful eyes demonstrated that the sharp contour of retinal elevation adjacent to the optic disc and inner retinoschisis-like separation (edema-like spaces) were reduced immediately, whereas in most eyes, the outer retinoschisis-like separation decreased slowly after vitrectomy. After reduction of the retinoschisis-like separation, the macular detachment decreased gradually with complete absorption of fluid after 6 to 16 months (average, 12 months; Figs 1 and 2). As the RD slowly resolved, there was an increase in the amount of subretinal precipitates; this corresponded to a thickening of the photoreceptor outer segments (Figs 1 and 2). A limited defect in the outer segments of photoreceptors or the inner segment/outer segment line at the fovea remained even after persistent complete retinal

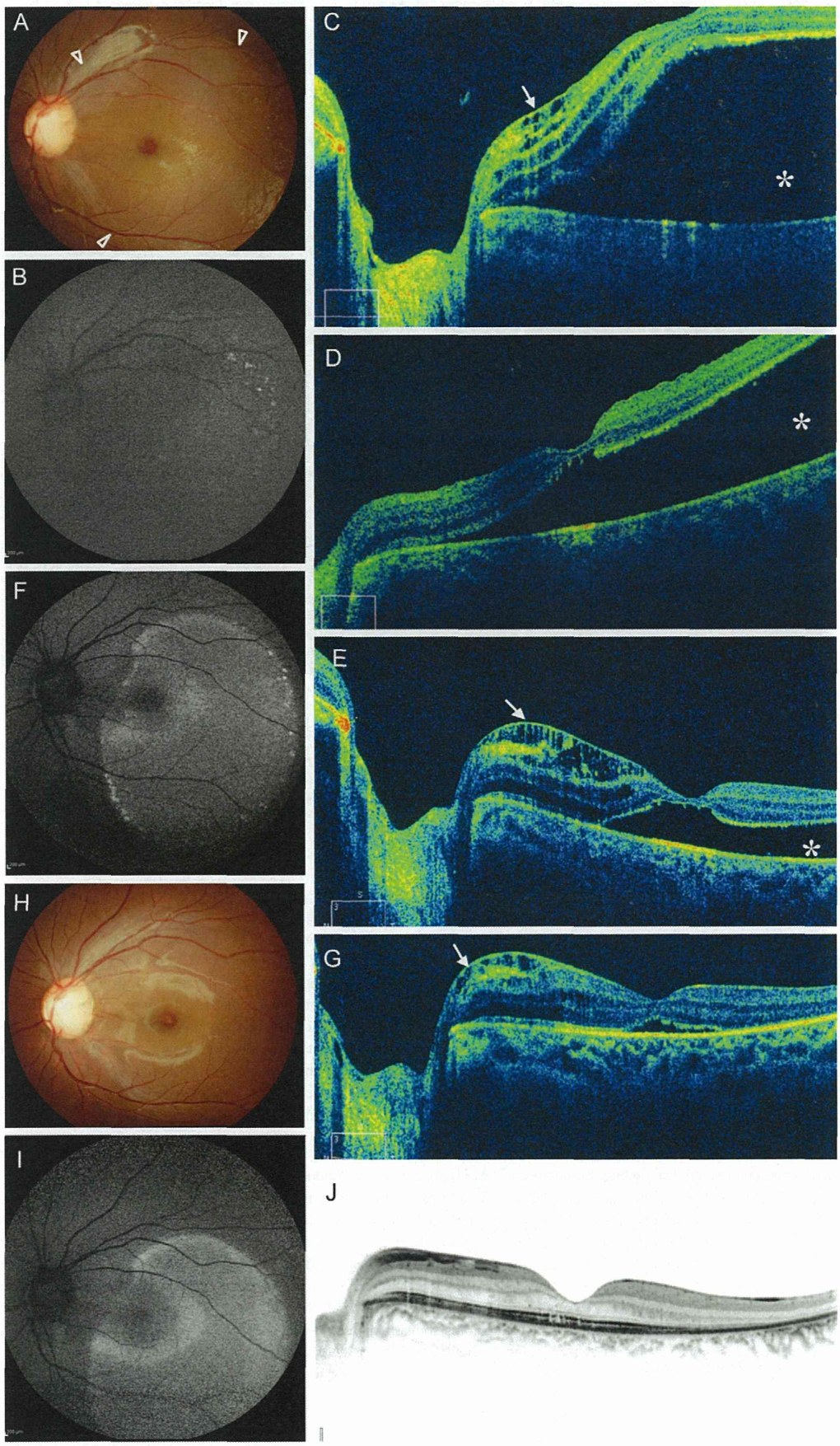
A
B
C
D
E
F
G
H
I
J

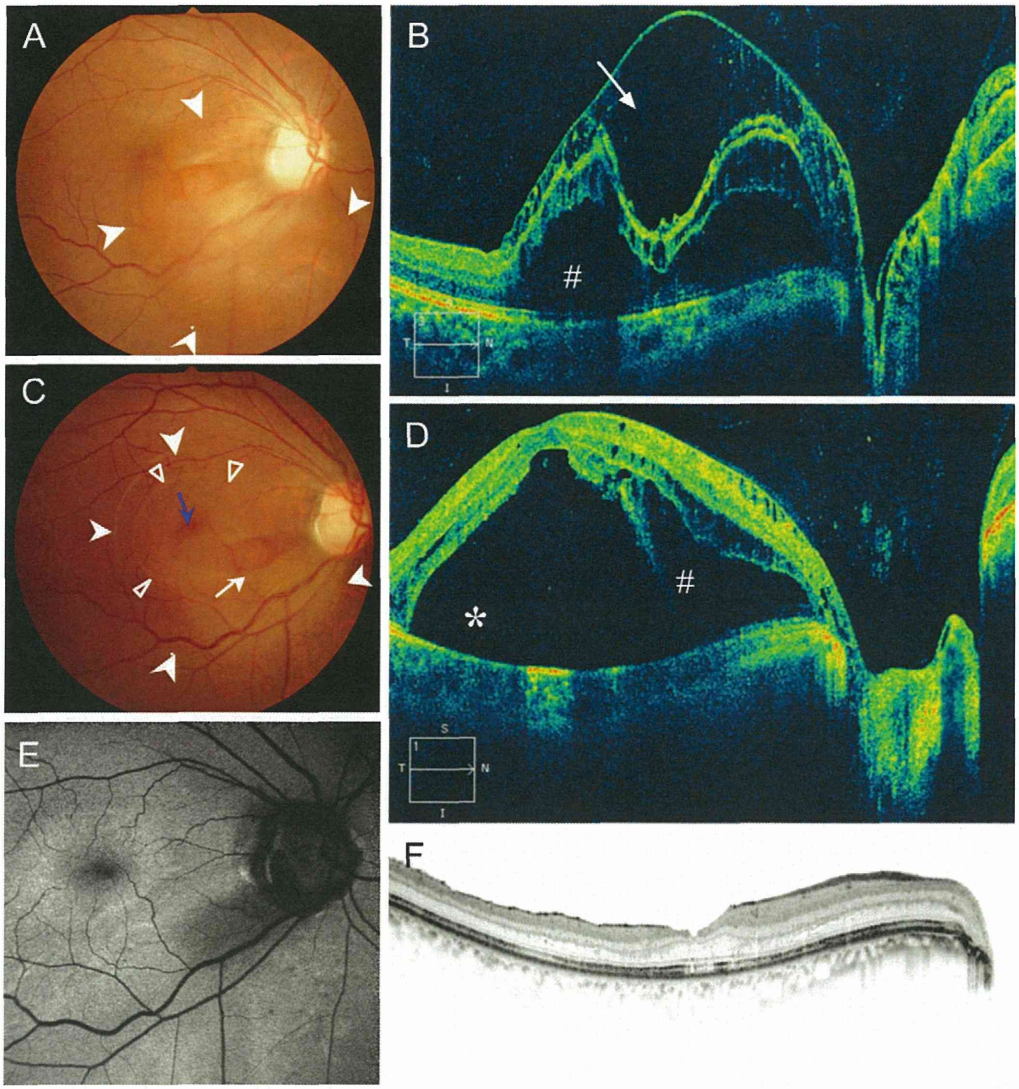

Figure 2. Composite of representative clinical findings from patient 8. **A,** Fundus photograph from the right eye obtained at the initial visit showing an inferotemporal optic disc pit associated with a large, round area of inferotemporal retinal elevation from optic disc (arrowheads). Before surgery, the best-corrected visual acuity (BCVA) was 20/17. **B,** Optical coherence tomography (OCT) scan obtained at the initial visit revealed a multilayered inner retinoschisis-like separation (#) with internal limiting membrane (ILM) detachment (arrow) connected to the optic disc pit. There was not retinal detachment. **C,** Preoperative photograph obtained at 2 months after the initial visit showing enlargement of retinal elevation beyond macula and appearance of round macular detachment (white open arrowheads). Tiny outer retinal break (blue arrows) and small area of shallow retinal with ILM separation (white arrow) were observed. The BCVA decreased to 20/50. **D,** Preoperative OCT scan revealing the development of retinal detachment (*) around the fovea and increased outer nuclear separation (#) with inner multilayers and retinoschisis-like separation between the optic disc and macula. **E,** Fundus autofluorescence image obtained 14 months after vitrectomy showing diffuse faint granular hyperfluorescence at the previous retinal detachment area. The BCVA was 20/20. **F,** Optical coherence tomography scan obtained 14 months after surgery showing improved complete retinal reattachment with tiny defect of the inner segment/outer segment line of the fovea.

Figure 1. Composite of representative clinical findings from patient 7. **A,** Photograph of left fundus before surgery showing a temporal optic disc pit associated with a large, round area of macular detachment (white open arrowheads). After surgery, the best-corrected visual acuity (BCVA) was 20/70. **B,** Preoperative fundus autofluorescence (FAF) image showing hypofluorescence in the area of retinal detachment. **C,** Optical coherence tomography scan obtained before surgery revealing a multilayered inner retinoschisis-like separation with internal limiting membrane (ILM) detachment (white solid arrow) and retinal detachment (*) present from the margin of the optic disc pit. **D,** Optical coherence tomography scan obtained on postvitrectomy day 1 showing a markedly decreased retinal detachment (*) and a shallowing of the retinoschisis-like separation next to the optic disc. The BCVA was 20/200. **E,** Optical coherence tomography scan obtained 6 months after vitrectomy: the retinoschisis-like separation and retinal detachment (*) were much decreased, but the ILM detachment between disc and macula remained (arrow). The BCVA was 20/70. **F,** Fundus autofluorescence image obtained 12 months after vitrectomy showing diffuse granular hyperfluorescence within the area of retinal detachment. **G,** Optical coherence tomography scan obtained 12 months after vitrectomy showing only a persistent shallow macular detachment. The outer segments of photoreceptors were thickening within the subfoveal lesion. Shallow ILM separation (arrow) beside the optic disc remained. The BCVA was 20/70. **H,** Fundus photograph obtained 16 months after surgery showing complete retinal reattachment with a clearer margin of optic disc pit. The BCVA was 20/30. **I,** Fundus autofluorescence image obtained 16 months after surgery showing fine granular hyperfluorescence at the site of previous retinal detachment. **J,** Optical coherence tomography scan obtained 16 months after surgery showing improvement in outer retinal anatomic features with a persistent defect in the inner segment/outer segment line at the fovea.

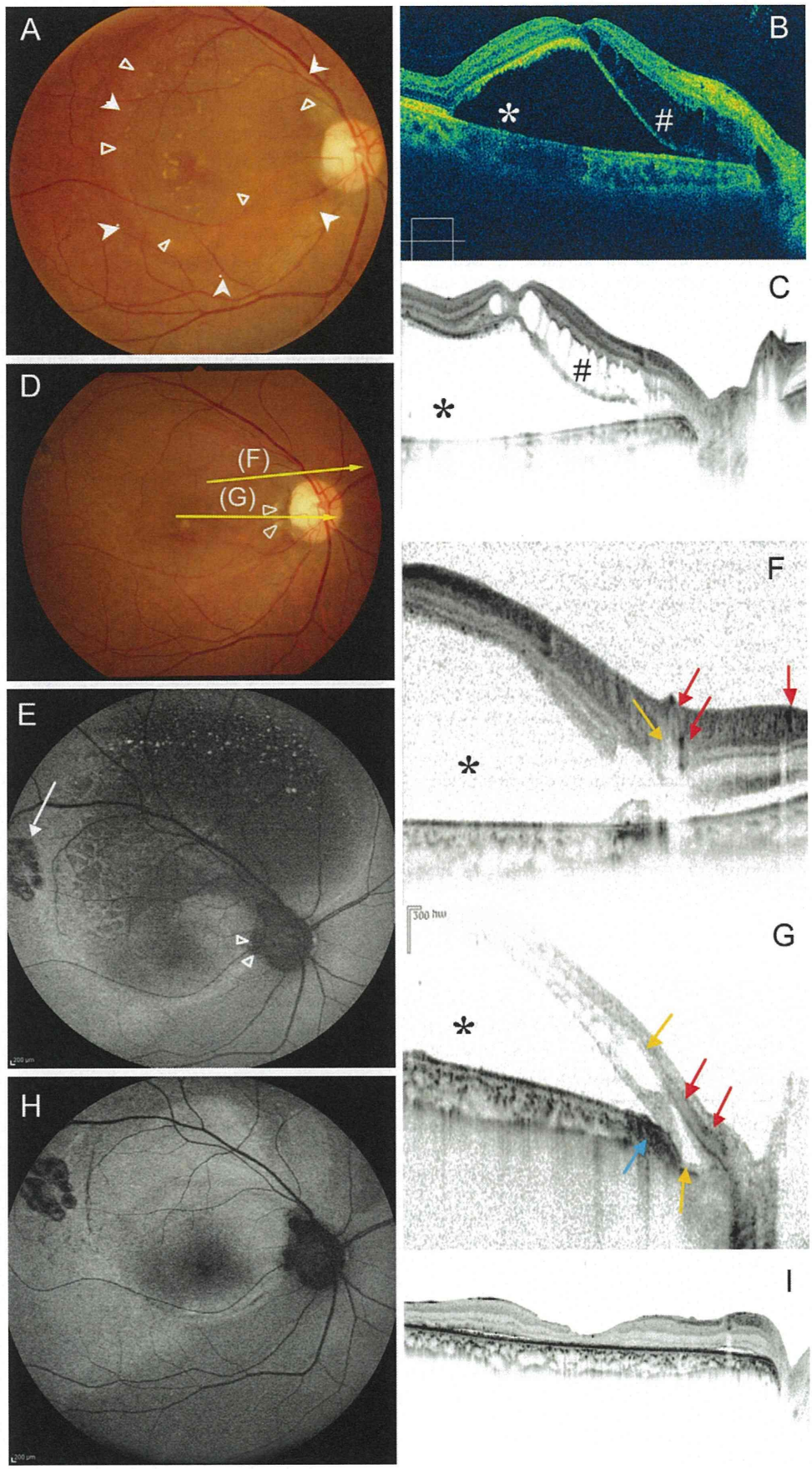
A
B
C
D
(F)
(G)
E
F
G
H
I

reattachment (Figs 1 and 2). The degree of excavation of the pits was not obvious before surgery; however, after surgery as the retina reattached, the pits were observed easily as being darker and deeper compared with the surrounding areas. The OCT images confirmed the increased depth of the excavation at the optic disc pit after vitrectomy in patients 1 and 7. Even after complete retinal reattachment, fine ILM elevation beside the optic disc remained in some eyes.

Visual Acuity Results

Preoperative and final BCVA are shown in Table 1. Despite evidence of some residual shallow schisis-like separation and some persistent macular detachment, the BCVA started to improve within a few months in all 7 successful eyes. This generally corresponded with reduced macular elevation and a better appearance of the photoreceptor outer segments on OCT. All eyes with retinal reattachment, except for patient 6 who needed additional treatment, had a postoperative BCVA of 20/30 or better. Although 3 eyes had a postoperative BCVA of 20/20 or better, a mild central scotoma or metamorphopsia remained. The BCVA of 1 eye (patient 6) started to improve after additional laser therapy and eventually reached 20/50.

Fundus Autofluorescence Findings

The FAF findings were obtained both before and after surgery in 3 eyes (patients 6, 7, and 8) and only after surgery in 1 eye (patient 4). Preoperative FAF images showed a prominent hypofluorescence corresponding to a high retinoschisis-like separation or macular detachment and a slight hypofluorescence corresponding to a shallow retinoschisis-like separation. After surgery, there was an increase in granular hyperfluorescence in FAF images accompanied by an increase in the amount of subretinal precipitates (Figs 1 and 2). This corresponded to a thickening of photoreceptor outer segments on OCT. Even after complete retinal reattachment, hyperfluorescence at the site of previous retinal detachment persisted through the most recent visit. In patient 6, the FAF images demonstrated an increase in granular hyperfluorescence with reduction of macular detachment after additional laser treatment (Fig 3).

Discussion

In this study, induction of a PVD without a gas tamponade seemed to be as effective as doing the same with a gas tamponade.[16] Optical coherence tomography revealed a reduction in the abrupt retinal elevation adjacent to the optic disc as well as a decrease in the inner retinoschisis-like separation in the early postoperative period. After reduction of the retinoschisis-like changes, there was a slow decrease in the macular retinal detachment, with complete resolution in 7 of 8 eyes within 16 months (average, 12 months; Figs 1 and 2). This pattern of improvement of macular elevation is similar to what was noted in a previous treatment using a gas tamponade.[16]

Bonnet[18] previously reported that none of the eyes with macular detachment in her series had evidence of a PVD and that the 2 eyes that demonstrated spontaneous reattachment did so after a PVD developed. In addition, Theodossiadis et al[19] described vitreous abnormalities such as vitreomacular traction and vitreous strands over the optic disc associated with optic disc pit maculopathy. In the current series, the sharp retinal elevation adjacent to the optic disc and inner retinoschisis-like separation immediately decreased after surgery, suggesting that traction on the peripapillary retina may be a trigger of optic disc pit maculopathy. Vitreoretinal traction is an important factor in the pathogenesis of optic disc pit maculopathy.

Recent advancements in OCT technology show that retinoschisis-like retinal separation is most prominent in the outer nuclear layers and frequently is combined with multiple shallow inner retinal separations.[19–21] A prominent elevation of the ILM has been reported in some eyes,[20] and a large, spontaneous separation of the ILM was observed before surgery in 1 eye (patient 8) in the current series. After surgery, shallow ILM detachment adjacent to the optic disc remained after complete retinal reattachment in some eyes. Similar to the original hypothesis of Lincoff et al,[5] in some, eyes schisis-like retinal separation preceded frank macular detachment with reduced vision.

Internal limiting membrane removal was performed in only 1 eye in this series. That eye (patient 8) had a spontaneous ILM detachment at presentation. There are some reports suggesting that ILM peeling is indicated during vitrectomy for optic disc pit maculopathy.[22–24] Internal limiting membrane removal ensures complete hyaloid removal. A partially separated ILM or ILM with cellular proliferation on its surface may contribute to peripapillary traction. Mac-

Figure 3. Composite of representative clinical findings from patient 6 (unsuccessful case). **A,** Right fundus photograph obtained before surgery showing an inferotemporal optic disc pit associated with a large, round macular elevation connected to the optic disc (large, solid arrows) and higher elevated macular detachment (white open arrowheads). The patient reported metamorphopsia, and the best-corrected visual acuity (BCVA) was 20/25. **B,** Preoperative optical coherence tomography (OCT) scan revealing a high separation of retinal detachment (*) with outer nuclear schisis-like separation (≠) and shallow internal limiting membrane elevation connected to the optic disc pit. **C,** Optical coherence tomography scan obtained 12 months after vitrectomy, when the patient reported decreased vision, revealing recurrence of retinoschisis-like separation at the outer nuclear layer (≠) and the worsening of retinal detachment (*). The BCVA decreased to 20/50. **D,** Fundus photograph obtained after additional treatment of gas tamponade and drainage of subretinal fluid, which did not work. Gas tamponade and laser photocoagulation were added to a small area beside the vessel in the peripapillary region (white open arrowheads). At 20 months after initial vitrectomy, subretinal fluid moved upward after laser treatment and decrease of macular detachment. The BCVA was 20/70. **E,** Fundus autofluorescence image obtained after the additional treatments at 20 months after initial vitrectomy revealing the laser spots around intentional break for the drainage of subretinal fluid (arrow) and beside the optic disc (white open arrowheads). The area of macular detachment started to increase the hyperfluorescence corresponding to the reduction of macular detachment and enlargement of hypofluorescence at the upper posterior retina corresponding to the high retinal elevation. **F–G,** Optical coherence tomography scan obtained during the follow-up after the additional treatment showing the subretinal space (*) connected to the perivascular space (yellow arrows) beside the retinal vessels (red arrows), especially around the optic disc. Laser scar next to the optic disc pit attached with neural retina (blue arrows). **H–I,** At 7 months after photocoagulation, **(H)** the image of FAF was the increase of hyperfluorescence **(I)** corresponding to macular reattachment by the OCT finding. The BCVA was 20/50.

Table 1. Preoperative Clinical Characteristics

Patient No.	Age (yrs)	Gender	Eye	Refractive Error (D)	Symptom	Preoperative Best-Corrected Visual Acuity	Pit Location	Duration of Symptoms (mos)	Outer Layer Schisis-like Separation
1	41	M	L	−2.75	Central scotoma	20/300	Inferotemporal	35	++
2	12	M	R	0	Decreased BCVA	20/40	Inferotemporal	28	++
3	20	M	L	0	Central scotoma	20/100	Temporal	10	−
4	56	M	L	−5.25	Central scotoma	20/100	Temporal	15	++
5	36	F	L	−1.25	Metamorphopsia	20/40	Temporal	3	++
6	47	F	R	+0.5	Metamorphopsia	20/25	Inferotemporal	18	+
7	8	M	L	−1.0	Decreased BCVA	20/70	Inferotemporal	2	+
8	38	M	R	0	Decreased BCVA	20/50	Inferotemporal	3	++

BCVA = best-corrected visual acuity; D = diopters; F = female; ILM = internal limiting membrane; L = left; M = male; R = right; + = present; ++ = remarkable finding; − = absent.
*Based on only time-domain optical coherence tomography observation.
†After first operation.
‡First, gas tamponade; second, internal limiting membrane peeling + subretinal fluid drainage + gas tamponade; third, laser (application).

ular schisis without an optic disc pit or resulting from high myopia has been reported,[25–29] suggesting that in some cases, vitreomacular traction can cause macular elevation resembling that resulting from optic disc pit maculopathy. The high degree of success noted in this series with careful and complete hyaloid removal as visualized with triamcinolone acetonide, however, suggests that ILM peeling is probably not essential in the treatment of most cases of optic pit maculopathy.

Previously, the authors reported that infrared and fundus autofluorescent images in optic disc pit maculopathy reflect the changes in the schisis-like separation and macular detachment corresponding with anatomic recovery,[30] Similar to Spaide,[31] it was found that FAF images developed brighter areas with increased granular hyperfluorescence corresponding to a thickening of photoreceptor outer segments on OCT after vitrectomy. This hyperfluorescence persisted for an extended period even after complete retinal reattachment. This FAF pattern during resolution of the macular detachment after vitreous surgery is very similar to the FAF images of chronic central serous choriodopathy.[32]

The BCVA started to improve after surgery despite the continued, albeit decreased, presence of schisis-like separation and foveal detachment. Optical coherence tomography images suggested that the main difference in the macular detachment after surgery compared with before surgery was a more regular appearance of the photoreceptor outer segments, corresponding to areas of hyperfluorescence on FAF images. If the source of intraretinal or subretinal fluids derives from the optic disc pit, fluid currents should be necessary to separate the intraretinal and subretinal spaces. Vitrectomy to remove the traction around the entrance cavity may decrease fluid currents and better allow remodeling of photoreceptor outer segments and, ultimately, better visual function.

In 1 of 8 eyes in this series (patient 6), macular reattachment with vitrectomy alone failed. Revision of vitrectomy with ILM peeling and subretinal fluid drainage with gas tamponade was not sufficient to reattach the macula, and local laser treatment to a small area beside the vessel in the peripapillary region was added. This reduced the macular detachment and shifted the subretinal fluid to the superior area around superior arcade. This suggested that the fluid may have come along the vessels from the optic disc into the intraretinal areas. The perivascular space at the optic disc may be connected to the subarachnoid space, just like Virchow-Robin spaces in the brain,[33] and the eyes with optic disc pit maculopathy may have enlarged perivascular spaces. The fluid flow around the perivascular space is consistent with the induction of a dome-shaped ILM elevation in patient 8 and in previously reported cases.[20,23]

Histopathologic analysis of optic disc pits reveals perineural herniation of poorly differentiated retinal tissue combined with vitreous collagen around the optic nerve into the subarachnoid space.[34] In our cases, vitrectomy with induction of a PVD led to deepening of the excavation of the pit. There may be transparent neural tissue in the pit separating the vitreous cavity from the subarachnoid space.[35] The pit is porous because of the disorganized tissue, and the lamina cribrosa also is defective within the pit.[34] Intracranial pressure and intraocular pressure both fluctuate, although intraocular pressure is usually greater than intracranial pressure. When intraocular pressure is greater, vitreous fluid moves into the pit sac. When intracranial pressure is greater, depending on the body position, for example, some fluid in the sac may be pushed back into the eye through the pit. However, some fluid in the sac also could move into the retina, leading to a retinoschisis-like separation. The authors believe that this dynamic fluid movement in the pit sac like is an eddy where there is turbulent flow. The turbulent flow contributes to the enlargement of the pit sac or perivascular spaces and is the cause of the schisis-like separation. When there is posterior hyaloid traction caused by age-related vitreous liquefaction or trauma, it pulls on the optic disc pit. Because the pit is pulled up like a tent by vitreous traction, the turbulent flow may have increased access around the vessels to the intraretinal space. This traction affects the peripapillary retina, especially around the pit. This further facilitates intraretinal fluid accumulation. When a PVD occurs, the anterior traction is released. The pit decompresses and moves down-

and Outcomes of Vitrectomy

Inner Layer Separation	Retinal Detachment	ILM Detachment	Outer Layer Break	Posterior Vitreous Detachment	Time to Macular Attachment (mos)	Additional Treatment	Most Recent Best-Corrected Visual Acuity	Follow-up (mos)
−*	+	−	+	−	14	−	20/17	35
+	++	−	+	−	10	−	20/17	46
−	+	−	−	−	10	−	20/30	10
+	+	−	+	−	15	−	20/30	35
−*	−	−	−	−	6	−	20/25	18
+	++	−	−	−	24†	+(3 times)‡	20/50	24
+	++	+	−	−	16	−	20/30	20
+	+	+	+	−	12	−	20/20	16

ward, and access to the subretinal space becomes limited. Any traction on the peripapillary retina also is released.

During induction of a PVD, a tight adhesion of the posterior hyaloid or abnormal membrane, such as anomalous Cloquet's canal, to the margin of the disc pit has been reported.[36,37] The authors have observed during surgery a posterior hyaloid strand tightly attached to the optic disc pit using triamcinolone acetonide that was sucked into the pit as a PVD was created,[36] suggesting that the unusual movement of fluid between the vitreous cavity and subarachnoid space and traction around the posterior hyaloid may contribute to the pathogenesis of this disease.

In conclusion, vitrectomy with induction of a PVD without a gas tamponade or laser photocoagulation allows resolution of optic disc pit maculopathy in most cases. Treatment without a gas or silicone oil tamponade avoids intraoperative and postoperative complications related to the tamponading agent.[16,38,39] This study suggests that peripapillary vitreous traction is the trigger of the schisis-like separation and that the perivascular space around the optic disc pit allows for the passage of fluid into the retina associated with optic disc pit maculopathy.

References

1. Wiethe T. Ein Fall von angeborener Difformitat der Sehnervenpapille. Arch Augenheilkd 1882;11:14–9.
2. Kranenburg EW. Crater-like holes in the optic disc and central serous retinopathy. Arch Ophthalmol 1960;64:912–24.
3. Brown GC, Shields JA, Goldberg RE. Congenital pits of the nerve head: II. Clinical studies in humans. Ophthalmology 1980;87:51–65.
4. Sobol WM, Blodi CF, Folk JC, Weingeist TA. Long-term visual outcome in patients with optic nerve pit and serous retinal detachment of the macula. Ophthalmology 1990;97:1539–42.
5. Lincoff H, Lopez R, Kreissig I, et al. Retinoschisis associated with optic nerve pits. Arch Ophthalmol 1988;106:61–7.
6. Rutledge BK, Puliafito CA, Duker JS, et al. Optical coherence tomography of macular lesions associated with optic nerve head pits. Ophthalmology 1996;103:1047–53.
7. Krivoy D, Gentile R, Liebmann JM, et al. Imaging congenital optic disc pits and associated maculopathy using optical coherence tomography. Arch Ophthalmol 1996;114:165–70.
8. Lincoff H, Kreissig I. Optical coherence tomography of pneumatic displacement of optic disc pit maculopathy. Br J Ophthalmol 1998;82:367–72.
9. Gass JD. Serous detachment of the macula: secondary to congenital pit of the optic nervehead. Am J Ophthalmol 1969;67:821–41.
10. Gass JD. Stereoscopic Atlas of Macular Diseases: Diagnosis and Treatment. 3rd ed. vol II. St. Louis, MO: Mosby; 1987:728–33.
11. Tobe T, Nishimura T, Uyama M. Laser photocoagulation for pit-macular syndrome [in Japanese]. Ganka Rinsho Iho 1991;85:124–30.
12. Cox MS, Witherspoon CD, Morris RE, Flynn HW. Evolving techniques in the treatment of macular detachment caused by optic nerve pits. Ophthalmology 1988;95:889–96.
13. Postel EA, Pulido JS, McNamara JA, Johnson MW. The etiology and treatment of macular detachment associated with optic nerve pits and related anomalies. Trans Am Ophthalmol Soc 1998;96:73–88.
14. Theodossiadis GP. Treatment of maculopathy associated with optic disk pit by sponge explant. Am J Ophthalmol 1996;121:630–7.
15. Lincoff H, Yanuzzi L, Singerman L, et al. Improvement in visual function after displacement of the retinal elevations emanating from optic pits. Arch Ophthalmol 1993;111:1071–9.
16. Hirakata A, Okada AA, Hida T. Long-term results of vitrectomy without laser treatment for macular detachment associated with an optic disc pit. Ophthalmology 2005;112:1430–5.
17. Sakamoto T, Miyazaki M, Hisatomi T, et al. Triamcinolone-assisted pars plana vitrectomy improves the surgical procedures and decreases the postoperative blood-ocular barrier breakdown. Graefes Arch Clin Exp Ophthalmol 2002;240:423–9.
18. Bonnet M. Serous macular detachment associated with optic nerve pits. Graefes Arch Clin Exp Ophthalmol 1991;229:526–32.
19. Theodossiadis PG, Grigoropoulos VG, Emfietzoglou J, Theodossiadis GP. Vitreous findings in optic disc pit maculopathy based on optical coherence tomography. Graefes Arch Clin Exp Ophthalmol 2007;245:1311–8.

20. Imamura Y, Zweifel SA, Fujiwara T, et al. High-resolution optical coherence tomography findings in optic pit maculopathy. Retina 2010;30:1104–12.
21. Lalwani GA, Punjabi OS, Flynn HW, et al. Documentation of optic nerve pit with macular schisis-like cavity by spectral domain OCT. Ophthalmic Surg Lasers Imaging 2007;38:262–4.
22. Georgalas I, Petrou P, Koutsandrea C, et al. Optic disc pit maculopathy treated with vitrectomy, internal limiting membrane peeling, and gas tamponade: a report of two cases. Eur J Ophthalmol 2009;19:324–6.
23. Spaide RF, Fisher Y, Ober M, Stoller G. Surgical hypothesis: inner retinal fenestration as a treatment for optic disc pit maculopathy. Retina 2006;26:89–91.
24. Ishikawa K, Terasaki H, Mori M, et al. Optical coherence tomography before and after vitrectomy with internal limiting membrane removal in a child with optic disc pit maculopathy. Jpn J Ophthalmol 2005;49:411–3.
25. Yamada N, Kishi S. Tomographic features and surgical outcomes of vitreomacular traction syndrome. Am J Ophthalmol 2005;139:112–7.
26. Gallemore RP, Jumper JM, McCuen BW II, et al. Diagnosis of vitreoretinal adhesions in macular disease with optical coherence tomography. Retina 2000;20:115–20.
27. Spaide RF, Costa DL, Huang SJ. Macular schisis in a patient without an optic disk pit optical coherence tomographic findings. Retina 2003;23:238–40.
28. Takano M, Kishi S. Foveal retinoschisis and retinal detachment in severely myopic eyes with posterior staphyloma. Am J Ophthalmol 1999;128:472–6.
29. Ikuno Y, Sayanagi K, Ohji M, et al. Vitrectomy and internal limiting membrane peeling for myopic foveoschisis. Am J Ophthalmol 2004;137:719–24.
30. Hiraoka T, Inoue M, Ninomiya Y, Hirakata A. Infrared and fundus autofluorescence imaging in eyes with optic disc pit maculopathy. Clin Experiment Ophthalmol 2010;38:669–77.
31. Spaide R. Autofluorescence from the outer retina and subretinal space: hypothesis and review. Retina 2008;28:5–35.
32. Kon Y, Iida T, Maruko I, Saito M. The optical coherence tomography-ophthalmoscope for examination of central serous chorioretinopathy with precipitates. Retina 2008;28:864–9.
33. Doubal FN, MacLullich AMJ, Ferguson KF, et al. Enlarged perivascular spaces on MRI are a feature of cerebral small vessel disease. Stroke 2010;41:450–4.
34. Irvine AR, Crawford JB, Sullivan JH. The pathogenesis of retinal detachment with morning glory disc and optic pit. Retina 1986;6:146–50.
35. Johnson TM, Johnson MW. Pathogenic implications of subretinal gas migration through pits and atypical colobomas of the optic nerve. Arch Ophthalmol 2004;122:1793–800.
36. Hirakata A, Hida T, Wakabayashi T, et al. Unusual posterior hyaloid strand in a young child with optic disc pit maculopathy: intraoperative and histopathological findings. Jpn J Ophthalmol 2005;49:264–6.
37. Akiba J, Kakehashi A, Hikichi T, Trempe CL. Vitreous findings in cases of optic nerve pits and serous macular detachment. Am J Ophthalmol 1993;116:38–41.
38. Kuhn F, Kover F, Szabo I, Mester V. Intracranial migration of silicone oil from an eye with optic pit. Graefes Arch Clin Exp Ophthalmol 2006;244:1360–2.
39. Pendergast SD, McCuen BW II. Visual field loss after macular hole surgery. Ophthalmology 1996;103:1069–77.

Footnotes and Financial Disclosures

Originally received: April 27, 2011.
Final revision: August 14, 2011.
Accepted: September 14, 2011.
Available online: January 14, 2012. Manuscript no. 2011-642.

[1] Department of Ophthalmology, Kyorin University School of Medicine, Tokyo, Japan.

[2] Department of Ophthalmology, Duke University School of Medicine, Durham, North Carolina.

Presented in part at the XXVII Meeting of the Club Jules Gonin, November 2010, Tokyo, Japan; and at the Annual Meeting of the Retina Society, September 2008, Scottsdale, Arizona.

Financial Disclosure(s):
The author(s) have no proprietary or commercial interest in any materials discussed in this article.

Correspondence:
Akito Hirakata, MD, Department of Ophthalmology, Kyorin University School of Medicine, 6-20-2 Shinkawa, Mitaka, Tokyo 181-8611 Japan. E-mail: hirakata@eye-center.org.

Significant Correlation Between Visual Acuity and Recovery of Foveal Cone Microstructures After Macular Hole Surgery

YUJI ITOH, MAKOTO INOUE, TOSHO RII, TOMOYUKI HIRAOKA, AND AKITO HIRAKATA

• PURPOSE: To determine whether a recovery of the microstructures of the foveal photoreceptors after macular hole closure is correlated with best-corrected visual acuity (BCVA).

• DESIGN: Retrospective, consecutive, observational case series.

• METHODS: SETTING: Single-center academic practice. STUDY POPULATION: Forty-one eyes of 41 patients with surgically closed macular holes. OBSERVATIONAL PROCEDURES: The presence and intactness of the cone outer segment tips (COST) line were determined by spectral-domain optical coherence tomography and compared with the presence of the inner segment/outer segment (IS/OS) junction and the external limiting membrane (ELM) at 1, 3, 6, 9, and 12 months after the macular hole surgery. MAIN OUTCOME MEASURE: The correlation between the integrity of the foveal photoreceptor microstructures and the BCVA.

• RESULTS: A distinct COST line was first seen at 6 months after the surgery. A distinct or irregular COST line was observed only in eyes with an intact IS/OS junction and ELM. Eyes with a distinct or irregular COST line had significantly better BCVA than those with a disrupted COST line in eyes with an intact IS/OS junction and ELM at 12 months ($P = .030$). The BCVA was ≥20/25 at 12 months in 91% of the eyes with a distinct or irregular COST line but in only 44% of the eyes without a COST line ($P = .015$).

• CONCLUSIONS: The significant correlation between the BCVA and a distinct or irregular COST line after successful macular hole surgery indicates that the recovery of foveal cone microstructure is associated with good postoperative BCVA. (Am J Ophthalmol 2012;153: 111–119. Crown Copyright © 2012 Published by Elsevier Inc. All rights reserved.)

AN IDIOPATHIC MACULAR HOLE CAN BE SUCCESSfully closed by vitreous surgery with recovery of good vision. However, the degree of visual recovery varies, and some cases do not recover good vision despite the closure of the macular hole.[1–9] In addition, the duration for the visual recovery varies considerably and can be long.[8,9] The factors that are related to the recovery of vision postoperatively have not been determined.

Spectral-domain optical coherence tomography (SD-OCT) has allowed investigators to evaluate the microstructures of the photoreceptors noninvasively in eyes with different types of retinal diseases, including those with idiopathic macular holes.[10] Several studies have shown that the restoration of the photoreceptor inner segment/outer segment (IS/OS) junction was significantly correlated with the recovery of visual acuity after surgery.[11–18] This significant correlation has also been found in cases of epiretinal membrane,[19] diabetic macular edema,[20,21] rhegmatogenous retinal detachment,[22,23] retinal vein occlusion,[24] and age-related macular degeneration.[25] It was suggested that the presence of a continuous IS/OS line was a sign of well-restored photoreceptor cells,[23] and a continuous external limiting membrane (ELM) was a sign of intact photoreceptor cell bodies and Müller cells.[22,26] These findings indicated that both the ELM and IS/OS junction can recover but the IS/OS junction rarely recovered without a recovery of the ELM.[26]

High-speed, ultrahigh-resolution optical coherence tomography (UHR-OCT) has been used to acquire, measure, and map the outer retinal morphology including the topographic distribution of cones and rods in the macula.[27] A bright back-reflecting line located between the IS/OS junction and retinal pigment epithelium in the UHR-OCT images has been identified as the boundary of the cone outer segment tips (COST).[27] The relationship between visual acuity and the integrity of the foveal COST line detected by commercially available SD-OCTs has been reported in cases of occult macular dystrophy.[28] We performed a preliminary study of 37 eyes of 37 normal subjects, and a distinct COST line was detected in over 94% of the Cirrus SD-OCT images with the 5-line raster mode (unpublished data).

We hypothesized that the postoperative recovery of visual acuity is dependent on the restoration of the foveal COST line. To test this hypothesis, we determined the correlation between the best-corrected visual acuity (BCVA) and the integrity of the foveal COST line, the IS/OS junction, and the ELM in the SD-OCT images.

Accepted for publication May 20, 2011.

From Kyorin Eye Center, Kyorin University School of Medicine, Tokyo, Japan.

Inquiries to Makoto Inoue, Kyorin Eye Center, Kyorin University School of Medicine, 6-20-2 Shinkawa, Mitaka, Tokyo, 181-8611, Japan; e-mail: inoue@eye-center.org

0002-9394/$36.00
doi:10.1016/j.ajo.2011.05.039

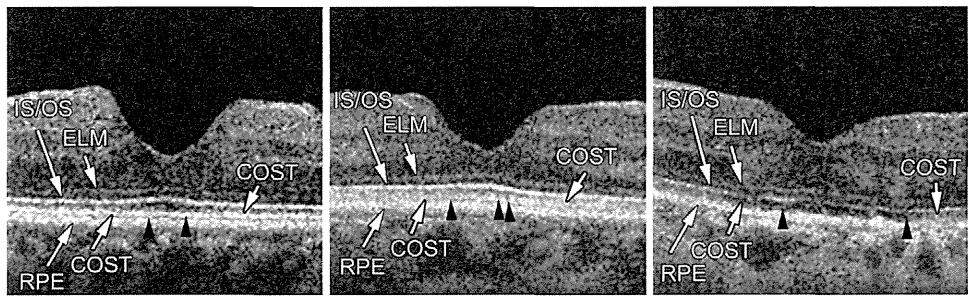

FIGURE 1. Spectral-domain optical coherence tomographic (SD-OCT) images showing the photoreceptor cone outer segment tips (COST) line of the foveal cone microstructures after macular hole surgery. (Left) COST line (arrowheads) is distinct and continuous (COST+; arrowheads). (Middle) COST line is irregular and disrupted (COST+; arrowheads). (Right) COST line is absent (arrowheads) at the fovea (COST-). ELM+ external limiting membrane; IS/OS+ inner segment/outer segment junction; RPE+ retinal pigment epithelium.

PATIENTS AND METHODS

THE MEDICAL RECORDS OF 58 EYES OF 58 CONSECUTIVE patients with surgically closed macular holes were reviewed. All of the patients had undergone surgery from March 11, 2008 to August 13, 2009 at the Kyorin Eye Center, and all were diagnosed with either a stage 2, 3, or 4 idiopathic macular hole according to the Gass classification. The preoperative data recorded included age, sex, right or left eye, axial length, stage of macular hole, the apical diameter of the macular hole before the operation determined by SD-OCT, and Snellen BCVA. The apical diameter was defined as the minimum distance at the neurosensory retinal defect at the fovea in the vertical and horizontal images.

All of the patients had comprehensive ophthalmologic examinations preoperatively and 1, 3, 6, 9, and 12 months postoperatively. The examinations included BCVA, binocular indirect ophthalmoscopy, non-contact lens slit-lamp biomicroscopy, fundus photography, and fundus autofluorescence imaging by a confocal scanning laser ophthalmoscope (Heidelberg Retina Angiograph 2; Heidelberg Engineering, Heidelberg, Germany).

The SD-OCT examination was performed on all patients on the same day as the clinical examinations. The SD-OCT images were evaluated to determine the integrity of the ELM, IS/OS junction, and the COST line.

All surgeries were performed after the patients received a detailed explanation of the surgical and SD-OCT procedures. The main outcome measures were the 12-month-postoperative BCVA and the condition of the foveal microstructures in the SD-OCT images.

The surgery was performed by one of 3 retina specialists (T.H., M.I., A.H.). A standard 3-port pars plana vitrectomy was used to close the macular hole under 2% lidocaine retrobulbar anesthesia. An intravitreal injection of triamcinolone acetonide (Kenacort-A; Bristol Pharmaceuticals KK, Tokyo, Japan) or indocyanine green (Santen Pharmacy, Osaka, Japan) was used to make the vitreous gel and internal limiting membrane more visible. Core vitrectomy was performed with the creation of a posterior vitreous detachment if one was not present, and the internal limiting membrane was removed in all cases. All cataractous lenses were removed by phacoemulsification with an implantation of an intraocular lens. The lens was also extracted from all patients >55 years. Room air or nonexpansive 20% sulfur hexafluoride was used to tamponade the retina, and patients were instructed to maintain a facedown position for 3 to 4 days postoperatively.

Anatomic success was defined as the presence of a flat or closed macular hole at 1 month postoperatively confirmed by biomicroscopy and SD-OCT and the absence of autofluorescence at the site of the macular hole.

Microstructural images of the fovea were obtained by the SD-OCT (OCT4000; Cirrus HD-OCT, Carl Zeiss Meditec Inc, Dublin, California, USA). The entire macular area was scanned, and high-quality images of 6-mm scans were obtained with the 5-line raster mode. We used the horizontal or vertical 6-mm scans to evaluate the IS/OS junction, ELM, and COST lines. Three experienced investigators (Y.I., M.I., T.R.) were masked to the patients' information, including the postoperative period and the BCVA, when evaluating the SD-OCT images.

A recovered foveal microstructure in the photoreceptor layer was defined as a recovery of the continuous back-reflecting lines corresponding to the COST line, IS/OS junction, and the ELM line. The COST line at the fovea was classified into 3 grades according to the integrity of the foveal microstructures: distinct and continuous COST line, present but irregular and disrupted line (distinct COST line and irregular COST line was defined as COST+), and absent COST line (COST-) (Figure 1). The grade of COST line was compared to the integrity of the IS/OS junction and ELM lines: both IS/OS junction and ELM intact (IS/OS+/ELM+), IS/OS junction absent but ELM intact (IS/OS-/ELM+), and both IS/OS junction and ELM absent (IS/OS-/ELM-). In addition, the correlations between eyes with COST+ and the postoperative BCVA and between eyes with COST+ and the IS/OS+/ELM+ at postoperative 12 months were calculated.

The axial length was measured with the OA1000 (TOMEY Corp, Nagoya, Japan) preoperatively. For statis-

TABLE 1. Baseline Characteristics of Patients who Underwent Macular Hole Surgery

Numbers of eyes (patients)	41 (41)
Age (y), mean ± SD (range)	65.8 ± 7.2 (47–80)
Sex, no. (%)	
Male	15 (37%)
Female	26 (63%)
Eye, no. (%)	
Right	20 (49%)
Left	21 (51%)
Axial length (mm), mean ± SD	23.6 ± 1.2
Preoperative BCVA (logMAR), mean ± SD	0.57 ± 0.24
Sympton duration (months), mean ± SD (range)	4.6 ± 4.0 (1–18)
Preoperative stage, no. (%)	
Stage 2	11 (27%)
Stage 3	25 (61%)
Stage 4	5 (12%)
Preoperative diameter of the hole (μm), mean ± SD (range)	325 ± 172 (136–946)
Intravitreal gas tamponade during PPV, no. (%)	
Air	16 (39%)
Sulfur hexafluoride	25 (61%)
Combination of cataract surgery, no. (%)	36 (88%)

BVCA = best-corrected visual acuity; logMAR = logarithm of the minimal angle of resolution; PPV = pars plana vitrectomy; SD = standard deviation; y = years.

tical analysis, decimal BCVA was converted to the logarithm of minimal angle of resolution (logMAR).

To compare 2 groups, continuous data were analyzed using Student *t* tests, but Welch's *t* tests were used in cases of unequal variances. For multiple comparisons of 3 groups, continuous data were analyzed using 1-way analysis of variance, and Kruskal-Wallis tests were used when the data were not normally distributed. Forward stepwise regression analysis was performed to investigate the relationships between postoperative foveal microstructures and visual acuity at 12 months. The status of the ELM was not analyzed from the explanatory variables because the ELM of all cases was well restored at 12 months after surgery. Multivariate analysis was also used to determine whether the age, sex, symptom duration, and preoperative BCVA were significantly associated with the COST status at postoperative 12 months.

RESULTS

OF THE ORIGINAL 58 EYES, 9 EYES WERE EXCLUDED BECAUSE of the presence of other retinal diseases including a treated rhegmatogenous retinal detachment, diabetic retinopathy,

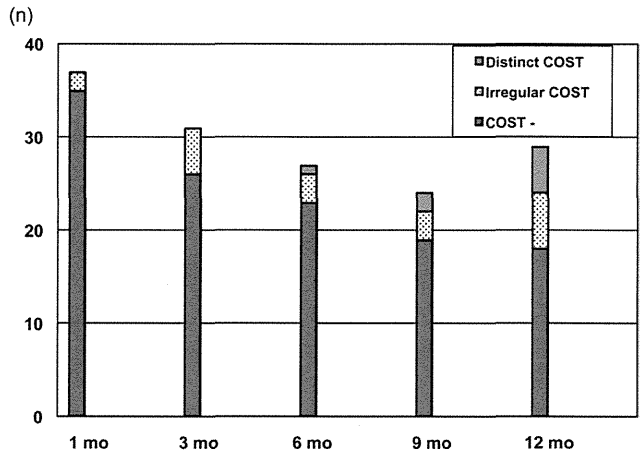

FIGURE 2. Spectral-domain optical coherence tomographic (SD-OCT) findings of foveal microstructures after macular hole surgery. Incidence of eyes with a distinct or an irregular photoreceptor cone outer segment tips (COST) line gradually increases, but the first distinct COST line is seen at 6 months while an irregular COST line is seen at 1 month.

and high myopia with an axial length > 27.0 mm, or refractive error < −8.0 diopters (D). Eight other eyes were excluded because they were followed for less than 6 months postoperatively. In the end, 41 eyes of 41 patients (15 men, 26 women) met the study criteria for the data analyses.

The preoperative baseline characteristics of the 41 eyes are summarized in Table 1. The mean age of the patients was 65.8 ± 7.2 years, with a range of 47–80 years. The average refractive error of the 38 phakic eyes was −1.5 D, with a range from −7.0 D to +3.5 D. The mean preoperative decimal BCVA was 0.27 (Snellen equivalent, 20/80; 0.57 logMAR units). The mean postoperative follow-up time was 11.0 months, with a range from 6 to 16 months. The interval between the onset of visual symptoms and the macular hole surgery ranged from 1 to 18 months, with a median of 4.6 months. The mean axial length of 39 of the eyes was 23.6 mm, with a range from 21.2 to 26.8 mm. The preoperative stage of the macular hole was stage 2 in 11 eyes (27%), stage 3 in 25 eyes (61%), and stage 4 in 5 eyes (12%).

The mean postoperative decimal BCVA was 0.50 (0.30 logMAR units) at 1 month, 0.62 (0.20 logMAR units) at 3 months, 0.65 (0.19 logMAR units) at 6 months, 0.75 (0.12 logMAR units) at 9 months, and 0.78 (0.11 logMAR units) at 12 months. Each postoperative BCVA was significantly better than the baseline BCVA ($P < .0001$, Student *t* tests).

• SPECTRAL-DOMAIN OPTICAL COHERENCE TOMOGRAPHY OF FOVEA: The integrity of the COST line was determined by SD-OCT (Figure 2). At 1 month, an irregular COST line was seen in 2 eyes (5%) and COST- in 35 (95%) of the 37 eyes examined. At 3 months,

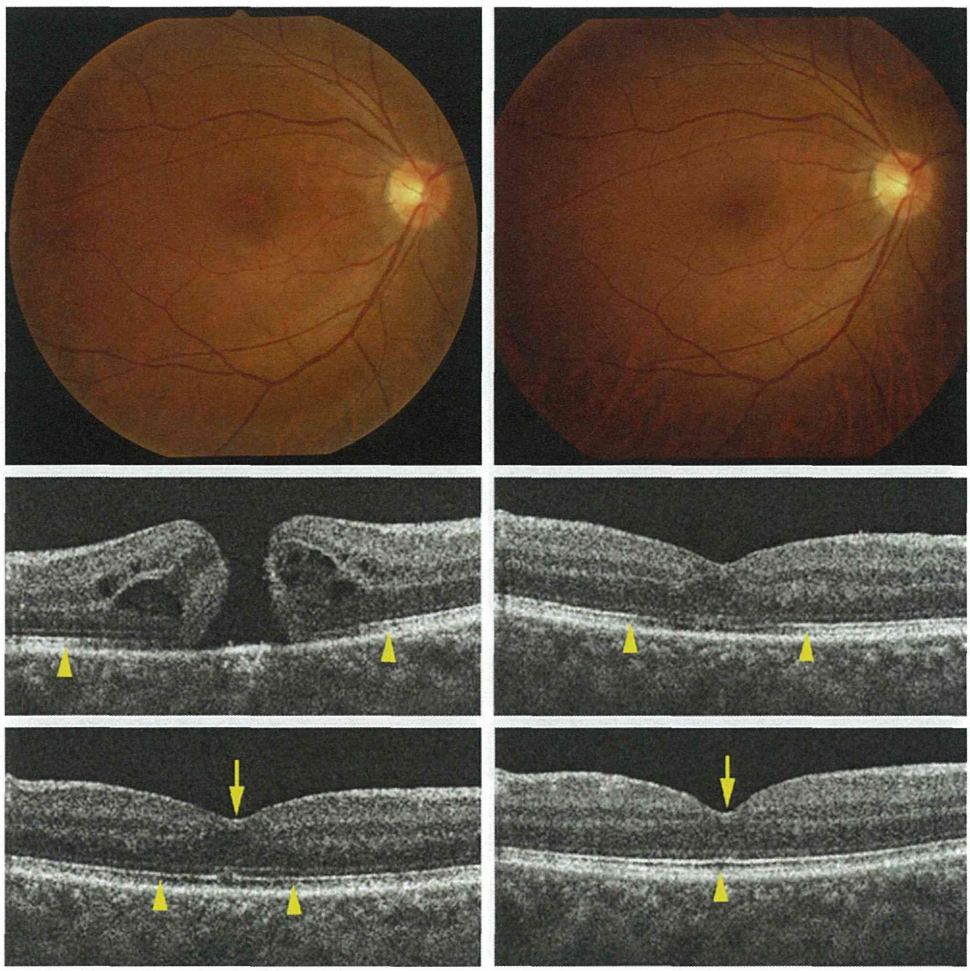

FIGURE 3. Preoperative and postoperative fundus photographs and spectral-domain optical coherence tomographic (SD-OCT) images of a 47-year-old man who underwent macular hole surgery. (Top left) Fundus photograph before surgery. The visual acuity (VA) was 20/40 in the right eye. (Top right) Fundus photograph of the closed macular hole 3 months after surgery. (Middle left) SD-OCT image obtained before surgery shows a full-thickness macular hole. The photoreceptor cone outer segment tips (COST) line is absent (yellow arrows) around the macular hole and the diameter of the COST defect is greater than that of the photoreceptor inner segment/outer segment (IS/OS) line and external limiting membrane (ELM) line. The diameter of the macular hole is 248 μm. (Middle right) SD-OCT image obtained 1 month after surgery shows a closed macular hole and incompletely restored IS/OS junction with a restored ELM. The COST line is absent (yellow arrows). (Bottom left) SD-OCT image obtained 3 months after surgery. The COST line is still absent (yellow arrowheads). The foveal hyper-reflective lesion (yellow arrow) indicates a decrease of signals of the intraretinal layer behind the lesion. (Bottom right) SD-OCT image obtained 12 months after surgery shows a restored COST line (yellow arrowhead) with restored IS/OS and ELM lines. The best-corrected VA improved to 20/22 at postoperative 12 months. The foveal hyper-reflective lesion (yellow arrow) indicates a decrease of signals of the intraretinal layer behind the lesion including the IS/OS and COST line.

an irregular COST line was seen in 5 eyes (16%) and COST- in 26 (84%) of 31 eyes. An eye with COST+ was first seen at 6 months along with an irregular COST line in 3 eyes (11%), and COST- in 23 (85%) of 27 eyes. At 9 months, a distinct COST line was seen in 2 eyes (8%), an irregular COST line in 3 eyes (13%), and COST- in 19 (79%) of the 24 eyes examined. At 12 months, a distinct COST line was seen in 5 eyes (17%), an irregular COST line in 6 eyes (21%), and COST- was seen in 18 (62%) of 29 eyes. The incidence of a distinct COST line gradually increased but the first appearance of a distinct COST line was later than that of IS/OS+.

The integrity of the IS/OS junction and the ELM was determined in a similar fashion. Thirty-seven eyes were examined 1 month after surgery, and IS/OS+/ELM+ was detected in 7 eyes (19%), IS/OS-/ELM+ in 9 eyes (24%), and IS/OS-/ELM- in 21 eyes (57%). The incidence of eyes with IS/OS+/ELM+ gradually increased and that of

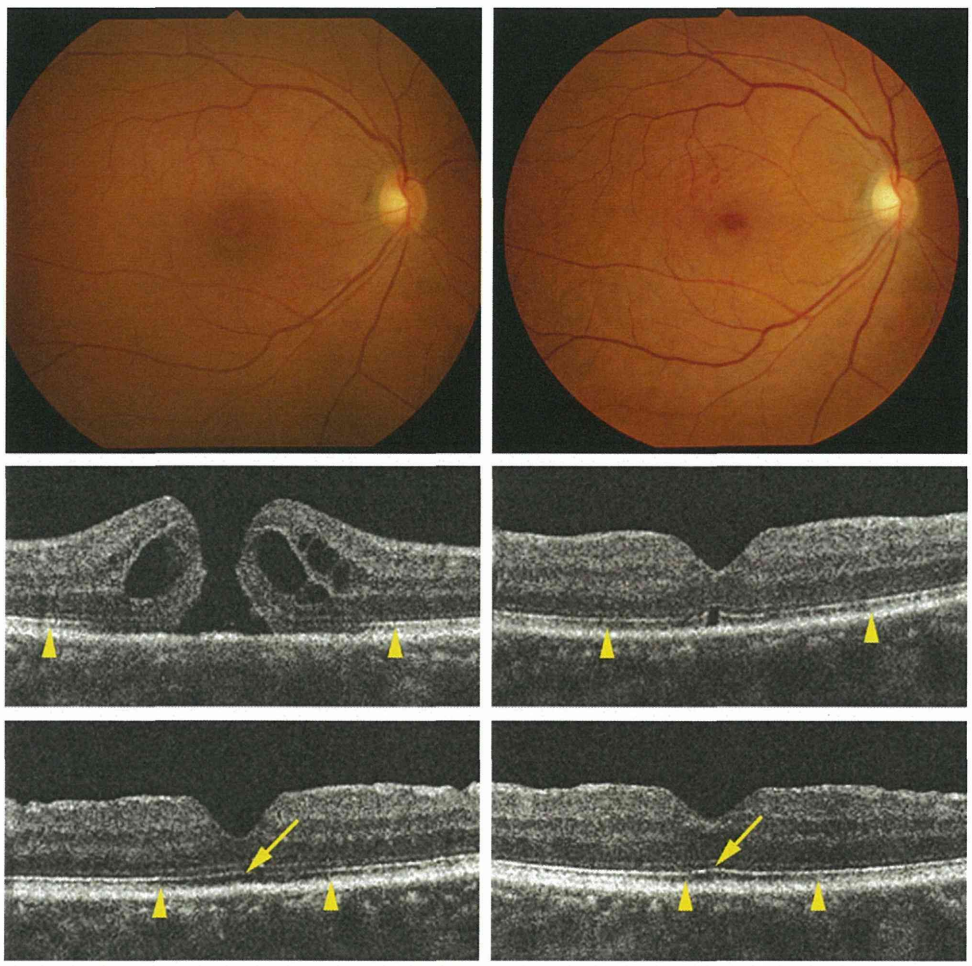

FIGURE 4. Preoperative and postoperative fundus photographs and spectral-domain optical coherence tomographic (SD-OCT) images of a 71-year-old man who underwent macular hole surgery. (Top left) Fundus photograph before surgery. The visual acuity (VA) was 20/60 in the right eye. (Top right) Fundus photograph of the closed macular hole 6 months after surgery. (Middle left) SD-OCT image obtained before surgery shows a full-thickness macular hole. The photoreceptor cone outer segment tips (COST) line is disrupted (yellow arrows) around the macular hole and the length of the COST line defect is larger than the defect of the photoreceptor inner segment/outer segment (IS/OS) junction and external limiting membrane (ELM). The diameter of the macular hole is 236 μm. (Middle right) SD-OCT image obtained 1 month after surgery shows a closed macular hole and partially disrupted IS/OS junction with a restored ELM. The COST line is absent (yellow arrows). (Bottom left) SD-OCT image obtained 3 months after surgery. The COST line is still absent (yellow arrowheads), although IS/OS (yellow arrow) and ELM lines are restored. (Bottom right) SD-OCT image obtained 12 months after surgery shows a disrupted COST line (yellow arrowhead) with restored IS/OS (yellow arrow) and ELM lines. The VA improved to 20/30 at postoperative 12 months.

IS/OS-/ELM- gradually decreased during the postoperative period. Twenty-nine eyes were examined at 12 months, and IS/OS+/ELM+ was seen in 23 eyes (79%) and IS/OS-/ELM+ in 6 eyes (21%). Eyes with IS/OS-/ELM- were not detected at 12 months after the surgery. Eyes with IS/OS+/ELM- were not seen at any postoperative period as reported.[26]

The SD-OCT findings showed that the COST line appeared only after the IS/OS junction and ELM had recovered (Figure 3), although the COST line did not fully recover even after the IS/OS junction and ELM had recovered in some patients (Figure 4).

• RELATIONSHIP BETWEEN SPECTRAL-DOMAIN OPTICAL COHERENCE TOMOGRAPHIC FINDINGS AND VISUAL ACUITY: The relationship between the presence of a COST line and the postoperative BCVA was determined (Figure 5). The BCVA of eyes with an irregular COST line was significantly better than that of eyes with COST- at 3, 6, and 9 months after the surgery. The eyes with a distinct COST line had significantly better BCVA than eyes with an irregular COST line or COST- at 12 months after the surgery.

Ten of 11 eyes with a postoperative BCVA ≥ 20/25 at 12 months had a distinct COST or irregular COST line

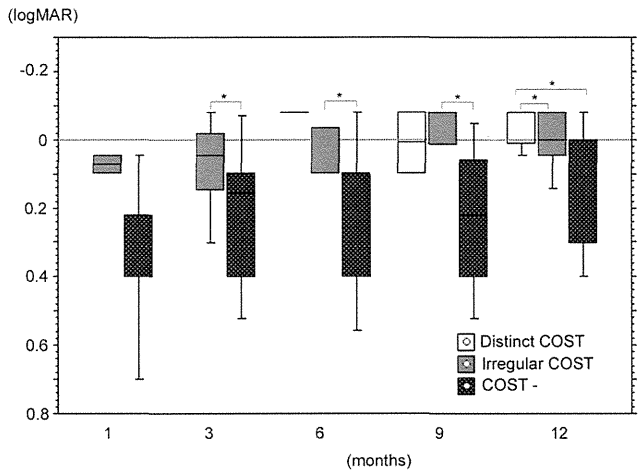

FIGURE 5. Foveal microstructures and postoperative best-corrected visual acuity (BCVA) after macular hole surgery. Distinct photoreceptor cone outer segment tips (COST) line first appears at 6 months after surgery and the BCVA of eyes with a distinct or irregular COST line is significantly better than that of other eyes at postoperative 12 months. * = $P < .05$, Kruskal-Wallis test and post-hoc test.

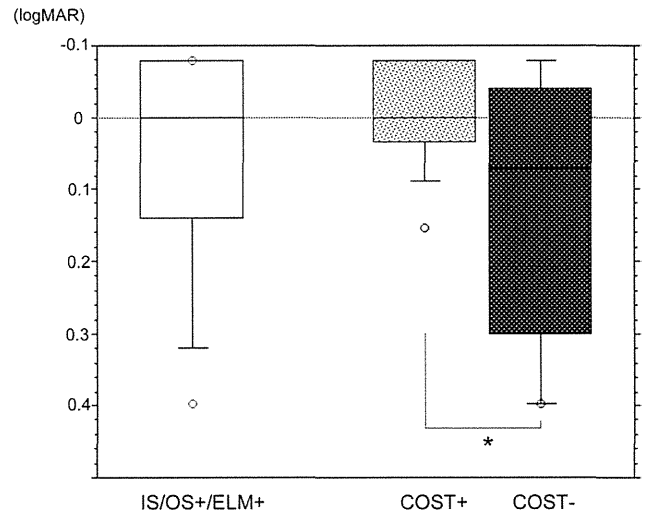

FIGURE 6. Foveal microstructures and postoperative best-corrected visual acuity (BCVA) in eyes with intact photoreceptor inner segment/outer segment (IS/OS) junction and external limiting membrane (ELM) lines at 12 months. The BCVA in eyes with IS/OS+/ELM+ varies considerably at 12 months. The postoperative BCVA is significantly better in eyes with COST+ than in eyes with COST- ($P = .030$, Welch's t test). COST = photoreceptor cone outer segment tips.

(COST+), which was significantly more than the 8 of 18 eyes with COST- ($P = .015$, Fisher exact probability test). The incidence of BCVA ≥ 20/25 in eyes with a distinct COST line was also significantly higher than that with COST- ($P = .038$), although the incidence of BCVA ≥ 20/25 in eyes with an irregular COST was not significantly different from that with COST- ($P = .188$). In eyes with well-restored IS/OS junction and ELM lines (IS/OS+/ELM+) at 12 months, the eyes with COST+ had significantly better BCVA than that of eyes with COST- (Figure 6, $P = .030$, Welch's t test). Eyes with a distinct or irregular COST line were observed only in eyes with IS/OS+/ELM+, and none of the eyes had a distinct or irregular COST line in the eyes with IS/OS-/ELM+ or IS/OS-/ELM-. These findings indicated that a recovery of the COST line after macular hole surgery was most likely responsible for the improvement of the BCVA.

• RELATIONSHIP BETWEEN PATIENTS' DEMOGRAPHICS AND COST LINE: The baseline demographics of the patients, intraoperative procedures, and BCVA at 12 months were compared between the 2 groups as a function of the integrity of the COST line at 12 months after surgery (Table 2). Forward stepwise regression analysis was performed to determine which variables were predictive of the COST line status at postoperative 12 months. One explanatory variable that was found to be significantly associated with the COST line status was symptom duration ($P = .029$). Age, sex, preoperative BCVA, axial length, preoperative diameter of the macular hole, and kind of intraoperative tamponade during surgery were not significantly associated. In addition, the postoperative BCVA at 12 months was significantly different between the 2 groups of COST+ and COST- ($P = .033$ Welch's t test).

Forward stepwise regression analysis was performed to investigate the relationship between postoperative COST line, IS/OS line status on SD-OCT, and visual acuity at 12 months. An explanatory variable that was found to be relevant to the BCVA at postoperative 12 months was the status of the COST line, but it was not found with the IS/OS line status. Standardized partial regression coefficients were assessed to discern the magnitude of each variable's influence. The integrity of the COST line status was more relevant (standardized partial regression coefficients; -0.398, F value = 4.894, $P = .036$) than the IS/OS line status (standardized partial regression coefficients; 0.0507, F value = 0.0671, $P = .798$) to the BCVA at postoperative 12 months.

DISCUSSION

TIME-DOMAIN OPTICAL COHERENCE TOMOGRAPHY (TD-OCT) instruments with a 10-μm axial resolution have been used to detect foveal retinal detachments, macular edema, and closure of a macular hole.[27] However, it is difficult to discriminate the foveal microstructures, including the irregularities of the IS/OS line and ELM, with these instruments. SD-OCT with a 5- to 6-μm axial resolution and UHR-OCT with a 3-μm resolution can detect these microstructures of the photoreceptors more clearly and more precisely.[10,22,27]

TABLE 2. Differences in Patient Characteristics Among Eyes Based on Cone Outer Segment Tips Line Status Detected by Spectral-Domain Optical Coherence Tomography at Postoperative 12 Months

Parameter	COST Line Status		*P* Value
	COST(+) (n = 11)	COST(-) (n = 18)	
Age (y), mean ± SD (range)	62.3 ± 8.3 (47-74)	67.3 ± 7.6 (54-80)	.472[a]
Preoperative BCVA			
LogMAR, mean ± SD	0.41 ± 0.1	0.55 ± 0.22	.576[a]
Postoperative BCVA at 12 months			
LogMAR, mean ± SD	−0.014 ± 0.076	0.17 ± 0.21	.033[b]
Symptom duration (months), mean ± SD	2.0 ± 0.6	6.5 ± 4.3	.029[a]
Axial length, mean ± SD	24.2 ± 1.4	23.5 ± 1.3	.583[a]
Preoperative apical diameter of hole (μm)			
Mean ± SD	283 ± 89	356 ± 212	.286[a]
Range	136–418	160–946	
Intravitreal tamponade during PPV, no. (%)			
Air	7 (64%)	7 (39)	.651[a]
Sulfur hexafluoride	4 (36%)	11 (61)	
Stage, no. (%)			
2	3 (27%)	6 (33%)	.075[c]
3	5 (46%)	11 (61%)	
4	3 (27%)	1 (6%)	

BCVA = best-corrected visual acuity; COST = cone outer segment tips; COST(+) = eyes with a distinct or irregular COST line at fovea; COST(−) = eyes without a COST line at fovea; logMAR = logarithm of minimal angle of resolution; PPV = pars plana vitrectomy; SD = standard deviation; y = years.

[a]Forward stepwise regression analysis.

[b]Welch's *t* test.

[c]χ^2 for independence test.

A restoration of the microstructures of the photoreceptors in the TD-OCT images has been proposed to be important for the recovery of good visual acuity after successful macular hole closure.[11,29] Specific microstructural characteristics have been used to determine the integrity of the photoreceptors in the SD-OCT images. Most of the earlier studies reported that the integrity of the photoreceptor IS/OS line was significantly correlated with postoperative visual acuity.[16–19] The photoreceptors are in a dynamic state of adding and shedding outer segments.[30] The foveal microstructures of the outer segments appear to be related to the functional status of the photoreceptors and related to visual acuity. However, other studies reported that the size of the disruption in the photoreceptor IS/OS junction was not correlated with postoperative BCVA.[12] The integrity of the IS/OS junction or the length of the foveal photoreceptor outer segments has been considered to indicate the functional status of the photoreceptors. However, the foveal IS/OS junction does not predict visual acuity after surgery because it is not a sign of the photoreceptor cell survival or rearrangement, which is probably more important in determining visual acuity. This may explain the contradictory visual outcomes reported in recent SD-OCT studies.[16,18,31]

The integrity of the ELM was reported to be another important morphologic structure of the photoreceptor layer that was related to visual acuity in patients with successful repair of a macular retinal detachment[22] and macular hole closure.[26] However, the BCVA in eyes with IS/OS+/ELM+ varied considerably at 12 months in our patients. We found that the eyes with COST+ had significantly better BCVA than those with COST- because of the presence of normally functioning cones.

Histopathologic and UHR-OCT analyses have shown that rods are absent in the foveola, and the cone outer segments extend to the retinal pigment epithelium apical surface.[27] The cone outer segment length is greatest in the foveola and decreases with increasing eccentricity.[27] Although there is a possibility that a COST line might not be detected by SD-OCT because of the resolution of commercially available SD-OCT, eyes with a distinct COST line in the SD-OCT images should have good BCVA. We do not have a suitable explanation of why the 8 eyes without COST signals could obtain better visual recovery (≥20/25) other than limited resolution of commercially available SD-OCT. However, the presence of a restored COST line is a potentially better indicator of good visual acuity than that of photoreceptor IS/OS junction and ELM.